The Journal of Foot & Ankle Surgery 59 (2020) 1306–1312

Contents lists available at ScienceDirect

The Journal of Foot & Ankle Surgery

journal homepage: www.jfas.org

Total Ankle Total Talus Replacement Using a 3D Printed Talus Component: A Case Report

Craig C. Akoh, MD[1], Jie Chen, MD, MPH[1], Samuel B. Adams, MD, FAOA, FAAOS[2]

[1] *Foot and Ankle Fellow, Duke University Medical Center, Durham, NC*
[2] *Assistant Professor, Duke University Medical Center, Durham, NC*

ARTICLE INFO

Level of Evidence: 4

Keywords:
additive manufacturing
ankle replacement
avascular necrosis
3D printing
osteonecrosis
total talus

ABSTRACT

The 3D custom total talus replacement is a novel treatment for avascular necrosis of the talus. However, patients who require a total talus replacement often have concomitant degenerative changes to the tibiotalar, subtalar, or talonavicular joints. The combined 3D custom total ankle-total talus replacement (TATTR) is used for patients with an unreconstructable talus and adjacent tibial plafond involvement. The goal of performing a TATTR is to provide pain relief, retain motion at the tibiotalar joint, maintain or improve the patient's functional status, and minimize limb shortening. TATTR is made possible by 3D printing. The advent of 3D printing has allowed for the accurate recreation of the native talar anatomy with a talar dome that can be matched to a total ankle replacement polyethylene bearing. In this article, we will discuss a case of talar avascular necrosis treated with a combined TATTR and review the current literature for TATTR.

There are various conditions that can lead to an unreconstructable talus, including but not limited to avascular necrosis (AVN), comminuted talus fracture, infection, tumors, and failed total ankle replacement (TAR). AVN is the most common reason for an unreconstructable talus. The prevailing etiology for talar AVN is a displaced talar neck fracture with up to a 60% risk of developing AVN (1,2). Other etiologies of AVN of the talus include excessive steroid use, alcohol, systemic lupus erythematosus, and chemotherapy drug use. With the increasing popularity of TAR, collapse of the talus under the talar component is becoming more prevalent. Catastrophic collapse of the talus does not allow for revision ankle replacement. Gross et al categorized the management of the unreconstructable talus into 4 categories: nonoperative, joint-sparing, surgical-salvage, and joint sacrificing treatments (3). Initial nonoperative treatment includes nonsteroidal anti-inflammatory drugs, bracing, protected weightbearing, extracorporeal shock wave therapy, and intraarticular injections. If nonoperative treatment fails, there are a variety of surgical treatment options for the unreconstructable talus depending on the severity of the condition. Joint sparing procedures include core decompression (4), talar allograft and vascularized autograft (5). Classically, pantalar arthrodesis with structural bone grafting has been the joint salvage procedure of choice (6). A staged pantalar arthrodesis may be indicated for infection and tumor cases. However, functional limitations, nonunion, and patient dissatisfaction have led patients and surgeons to seek alternative treatments (7-10). Below knee amputation is an option for an unsalvageable lower extremity (11).

The advent of patient-specific three-dimensional (3D) printing technology has allowed for the creation of digitally designed objects by sequential deposition of plastics, metal, or living cells (12). Metal additive manufacturing is commonly performed with titanium and cobalt-chromium (13). With an increased utilization of 3D printing within the orthopedic field, surgeons have shown improved surgical planning, implant design, and operative efficiency for complex foot and ankle pathologies (14-16). Its utilization gives the surgeon the ability to account for anatomic variability, various sizing options, and reduces the need for bone graft incorporation.

The first customized talar implants were reported in the literature in the 1990s as an alternative to arthrodesis procedures (17,18). This first-generation implant was a talar body only replacement made with either ceramic (17) or stainless-steel (18), with pegs cemented into the talar neck to provide initial fixation. Despite some early success, there were concerns of prosthesis loosening at the bone-peg interface and subtalar erosion due to sizing mismatch (18,19). As a result, second generation ceramic and metal talar body prosthesis were developed in the early 2000s without pegs and improved subtalar curvature, respectively. However, prosthesis loosening and talar head collapse continued to affect the survivorship of these implants (19,20). As a result, the custom ceramic total talus replacement (TTR) was developed in 2005 by

Financial Disclosure: None reported.
Conflict of Interest: Samuel B. Adams: Personal fees from Stryker, personal fees from Orthofix, personal fees from extremity medical, extremity fees from MedShape, personal fees from Exactech.

Address correspondence to: Craig C. Akoh, MD, Duke University Medical Center, Box 2887, Durham, NC 27710.
E-mail address: ccakoh@gmail.com (C.C. Akoh).

1067-2516/$ - see front matter © 2020 by the American College of Foot and Ankle Surgeons. All rights reserved.
https://doi.org/10.1053/j.jfas.2020.08.013

Taniguchi and has shown some favorable results for both ankle arthritis (21) and comminuted talar neck fractures (22).

In cases unreconstructable talar pathology and tibial-sided arthritic changes, there is a need for simultaneous total ankle-total talus replacement (TATTR) to optimize treatment. Currently, there are limited case series on metal TATTR (23-25) and single case series on ceramic prosthesis for TATTR (26). One study published by Kurokawa et al suggests that combined TATTR results in better clinical outcomes when compared to standard TAR for AVN of the talus. There is a lack of published literature describing the TATTR technique. The purpose of this article is to describe TATTR in the setting of unreconstructable talar pathology and ankle arthritis.

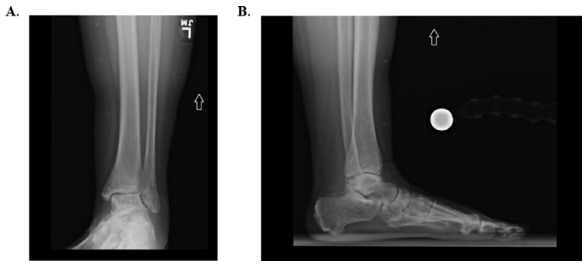

Fig. 1. Preoperative plain radiographs. Mortise (A) and lateral (B) plain radiographs of the left ankle shows talar AVN

Case Report

Our patient was a 59-year-old community ambulator female (body mass index 46.29 kg/m^2) with a history of immunoglobulin G (IgG) deficiency on chronic intravenous dexamethasone infusions that presented with severe left anterior ankle pain. She complained of ankle pain elicited with weight bearing. She had previously undergone conservative treatment such as nonsteroidal anti-inflammatory drugs, ankle brace, physical therapy, and a corticosteroid ankle injection. On examination, she was tender to palpation over her talus and tibiotalar joint. She had 20° of passive ankle dorsiflexion and 40° of plantarflexion. She was neurovascularly intact with intact motor strength. Three-view standing plain radiographs of the left ankle were obtained and showed severe talar dome sclerosis with early collapse (Fig. 1). Bilateral ankle standing computed tomography (CT) scans not only redemonstrated severe left talar dome sclerosis but also evidence of distal tibia bony infarct and lateral-sided cystic changes (Fig. 2A). Given the patient's recalcitrant pain and evidence of bony talar and tibial bony infarct changes, the patient was indicated for a TATTR.

Indications and Contraindications

Indications and contraindications for TATTR can be found on Table 1. Various indicated pathologies include advanced AVN, talar collapse, comminuted talus fracture, and talar-sided failure of a TAR. Of course on all situations of talus pathology, there must be tibial pathology include arthritis or even AVN of the pilon. Current absolute contraindications for a TATTR include active infection, irresectable tumor, neuropathic joint, noncorrectable ankle malalignment, AVN of the navicular, and AVN of the calcaneus. Relative contraindications include history of previous infection, pediatric patient, and deformity of the contralateral talus.

The surgeon must also evaluate the patient's talonavicular and subtalar joints for degenerative changes. Degenerative changes in these joints make the TATTR procedure more complicated. There is no data to determine if joint sparing or arthrodesis should be performed on the talonavicular or subtalar joints. Both joint sparing and arthrodesis options exist with 3D printing. Joint sparing can be performed with a 100% polished implant. Arthrodesis can be done using 3D printing technology by incorporating a porous osseointegration surface on these parts of the implant. In cases of subtalar and talonavicular degeneration, consideration should be given to TATTR with arthrodesis of these joints.

Table 1
Indications and contraindications

Indications	Contraindications
• Talar AVN with collapse and tibial-sided arthritis or AVN • Irreparable comminuted talus fracture	• Active infection • Unresectable tumor • Diabetic neuropathy • High-demand patient • Poor vascularity

The surgeon should provide informed consent with the patient to discuss risk, benefits, and alternatives to surgery. Potential complications associated with any foot and ankle procedure include infection, neurovascular injury, complex regional pain syndrome, and thromboembolic events (27). Specifically for TATAR procedures, potential complications include wound complications, periprosthetic fracture, prosthesis size mismatch, and instability (20,28,29) Kanzaki et al reported on their series of patients undergoing TATTR and their complications were delayed wound healing (13.6%) and medial malleolus fracture (18.1%). Other complications include adjacent joint degeneration of the subtalar and talonavicular joints, infection, and the possible need for a below-knee amputation. The patient must also have realistic expectations as lifestyle modifications are likely to occur after undergoing a TATTR. The patient should avoid heavy lifting, strenuous activities, and high-impact activities to prolong the longevity of the prosthesis and to minimize the likelihood of early failure.

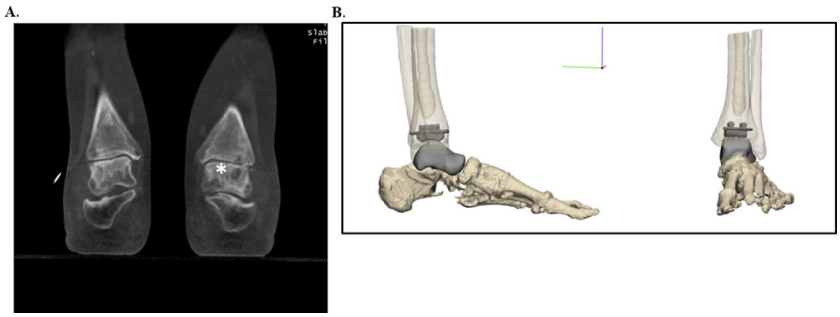

Fig. 2. Preoperative CT scan. Bilateral coronal CT (A) and 3D reconstruction (B) views. The 3D reconstruction imaging allows for preoperative planning and sizing of the total talar components. Note the tibial and Talar-sided cystic changes (asterisk)

Preoperative Planning

Preoperative planning is paramount for patients considering undergoing a TATTR. The treating surgeon should obtain a thorough history to determine the onset of pain as well as possible etiologies for talar pathology, especially in the case of AVN. The surgeon should perform a bilateral lower extremity examination on the patient to assess for tibiotalar joint pain, range of motion, and equinus contracture. Hindfoot alignment should be assessed to determine whether concomitant corrective procedures are needed. Probably more important with the TATTR than the TAR, the goal of restoring anatomic alignment is essential to keep the implant stable. A thorough neurovascular exam should also be performed to detect neuropathy or poor vascularity, which would preclude a patient from undergoing a TATTR.

Standard standing radiographic series of the foot (AP, lateral, and oblique) and ankle (AP, mortise, and lateral) should be obtained to assess deformity, presence of hardware, and adjacent joint pathology. A standing hindfoot Saltzman view is obtained if hindfoot deformity is suspected. Plain radiographs can also show tibiotalar joint space narrowing evidence of tibial-sided disease. If the plain radiographs suggest evidence of small focal talar necrosis without large subchondral cysts or collapse, then other joint-sparing procedures should be considered. In cases with talar AVN and subchondral collapse with preserved tibiotalar joint space, an isolated TTR should be considered.

Advanced imaging of the involved extremity should also be obtained to better characterize the extent of the talar dysvascularity as well as evidence of navicular, tibial, and calcaneal dysvascularity. Magnetic resonance imaging of the affected ankle will show evidence of hypointense signal of the talus on T1 and hyperintense signal on T2-weighted imaging, in cases of AVN. The integrity of the tibiotalar cartilage and subchondral bone can also be assessed on magnetic resonance imaging. Evidence of extensive bony infarct and AVN changes at the distal tibia warrants consideration of modular stemmed total ankle tibial prosthesis.

Bilateral ankle 3D reconstruction CT scans should be obtained during preoperative planning. CT scanning parameters are outlined on Table 2. CT scan of the operative ankle will allow the surgeon to quantify the amount of talar collapse and bone loss. A CT scan may also show cystic degeneration of the talus or demonstrate lack of adequate bone stock of the talus in cases of failed TAR. The surgeon can also evaluate the tibiotalar, talonavicular and subtalar joint for evidence of arthritis and need for concomitant arthrodesis procedures.

A CT scan of the contralateral ankle is imperative as the implant will be based of these anatomic data. The contralateral CT data will be "mirror imaged" to recreate the normal anatomy of the pathologic talus. The 3D printing company utilizes commercially available software that allows the design engineers to import the CT scan data, segment the anatomy, and create volumetric reconstructions for 3D printing of the metal implant (Fig. 2B). There is debate on the optimal metal for the TTR implant. Currently, the TTR portion of the TATTR can be made from polished cobalt-chromium or polished titanium with nitride coating.

It is also important that the surgeon provide the implant design engineers with the proposed tibial component manufacturer specifications so that the articulation of the custom 3D printed talus can match the polyethylene liner and tibial component. Of note, appropriate sizing of the implant may be challenging if the patient has bilateral talar AVN and collapse. In these cases, the surgeon should be intimately involved in the design process and should have several implant sizes prior to surgery. Metal artifact from existing hardware can also make reconstruction and segmentation of the anatomy more difficult. Reducing the slice spacing of the CT scan or removing the hardwire prior to the CT scan may be warranted.

Table 2
CT scan parameters

Parameter	Recommendation
File Type	DICOM
Field of View	Encompass all affected anatomy plus room for guide wrapping and / or implant fixation if applicable.
Pixel size	≤ 0.5 mm
Scan date	As recent as possible to avoid shifting and / or growing pathologies
Slice spacing	≤ 1.25 mm

Fig. 3. Total Talus Components. Trial total talus components (white components) and final trial components (metal) with 3 templated sizes for optimal fit

Selecting the appropriate-sized custom 3D-printed TTR for the TATTR can be difficult given multiple variables. We recommend for the surgeon's initial use, that the implant engineering team create 3 separate implants: (1) nominal (identical size to the contralateral talus), (2) small (5% smaller than the volumetric size of the nominal implant), and (3) large (5% larger than the volumetric size of the nominal implant; Fig. 3). As the surgeon becomes more familiar with the technique, the size options can be altered. Currently, Retor3d (Durham, NC), Additive Orthopaedics (Little Silver, NJ), and 4Web Medical (Frisco, TX) are the medical device companies which provide 3D printing services for TATTR.

Surgical Technique

A peripheral block was administered to the patient by the anesthesia team. The patient was then placed onto the operating table in the supine position with the foot at the end of the table. After securing the patient onto the operative table, a nonsterile thigh tourniquet is placed onto the operative extremity. An exam under anesthesia of both ankles was performed to compare the range of motion and stability of the operative and nonoperative sides. The goal of surgery was to replicate the range of motion and stability of the nonoperative side during the surgery. After standard prepping and draping, the operative extremity

Fig. 4. Anterior ankle approach. A standard anterior ankle approach is performed between the tibialis anterior and extensor hallucis longus tendons down to the anterior tibiotalar periosteum

is exsanguinated using a sterile Esmarch, and the tourniquet is inflated to 250-300 mm Hg to achieve adequate hemostasis.

A midline longitudinal anterior skin incision was made over the ankle 4 cm proximal to the tibiotalar joint and 2 cm distal to the navicular tuberosity (Fig. 4). Dissection was carried down through the subcutaneous tissues onto the extensor retinaculum. The superficial peroneal nerve was retracted laterally and protected. The extensor retinaculum is incised longitudinally at the interval between the tibialis anterior and extensor hallucis longus tendons. Scissor dissection should be used to locate the deep neurovascular structures so that they can be retracted laterally. The anterior ankle capsule is incised with a deep knife or electrocautery from the distal tibia to the talonavicular articulation and subperiosteally elevated while protecting the neurovascular bundle.

A large gelpi retractor was placed to maintain exposure of the anterior ankle. Once the tibiotalar and talonavicular joints were exposed, osteophytes were removed from the medial gutter, lateral gutter, and

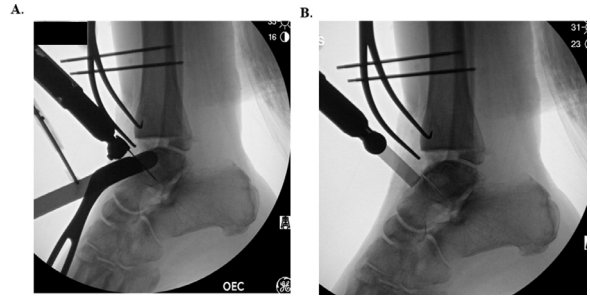

Fig. 6. Talus osteotomy. Talar neck coronal (*A*) and sagittal (*B*) osteotomy was performed with a small oscillating saw for the piecemeal removal of the native talus

anterior joint line using a rongeur. The surgeon should follow the TAR manufacturer's technique guide for tibia preparation. The tibial-sided preparation was performed prior to removing the talus to allow for more room to remove the talus and insert the TTR at later stages of the procedure (Fig. 5). The tibia plafond cut was made 2-3 mm more proximal than a normal cut to accommodate the total talus, polyethylene bearing, and tibial components. Care was made to protect the medial malleolus during the tibial cut.

Next, the native talus was removed in its entirety. During this part of the procedure, care was taken to perform all dissection of the capsule and ligaments from the talus as opposed to from the tibia, navicular, and calcaneus. Dissection from the pathologic talus allowed us to preserve the ligaments and capsular structures to contain the TATTR. The senior author prefers to remove the talus in 4 or more parts. A coronal plane osteotomy was made at the talar neck-dome junction with a small reciprocating saw under fluoroscopic guidance (Fig. 6). The talar osteotomy was completed with a 0.5-inch or 1.0-inch straight osteotome and advanced under fluoroscopic imaging to avoid damage to the subtalar articular cartilage. These same steps were then performed for a sagittal plane osteotomy of the talar neck. The coronal and sagittal plane osteotomies allowed for the neck pieces to be manipulated so that the interosseous ligament could be detached from the plantar aspect of the talus. A key elevator can be used to dissect the ligaments from the talar neck pieces.

Once the talar neck is removed, the talar body was fully visualized. Next, in a similar fashion as before, 1 or more sagittal plane osteotomies were made in the talar body with a saw under fluoroscopic imaging and then with an osteotome. Care was taken to not damage the posterior ankle structures. The talar body was carefully dissected from the deltoid ligament and posterior capsule while avoid injuring the medial malleolus. Once the talus was removed, the remaining small bony fragment was removed and the cavity was irrigated. Failing to remove the small fragments can prevent the proper reduction of the talar trial and

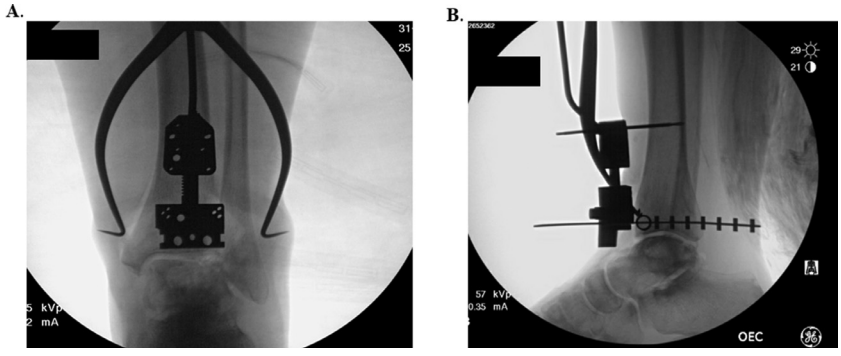

Fig. 5. Distal tibial resection. Intraoperative mortise (*A*) and lateral (*B*) views of the ankle with the extramedullary resection guide in place

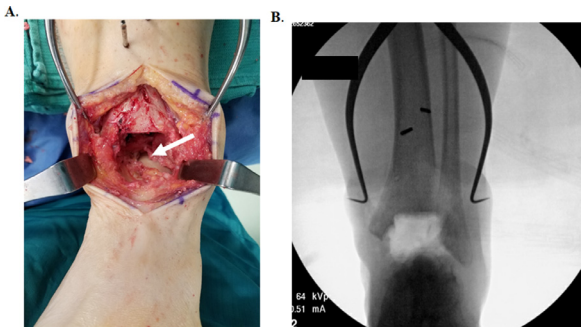

Fig. 7. Talar resection. Intraoperative clinical view of the ankle (*A*) and mortise (*B*) of the ankle after the native talar resection. Note the intact cartilage of the posterior facet of the calcaneus (white arrow)

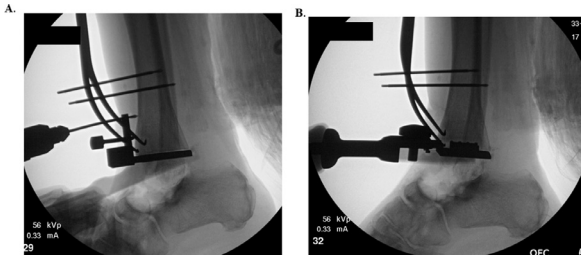

Fig. 8. Final tibial preparation. Lateral intraoperative fluoroscopic views of the ankle with the anterior tibial barrel guide (*A*) and final tibial component impaction (*B*)

malposition of the final component. The navicular and calcaneus cartilage were inspected to ensure there is no evidence of arthritis or iatrogenic damage (Fig. 7A). A fluoroscopic image was taken to confirm that the talus had been removed and that there were no signs of intraoperative fracture (Fig. 7B). After this, the remaining tibial preparation is performed (Fig. 8).

The trial 3D printed TTR trials were placed onto the calcaneus to help determine the correct size of the implant. Since the tibia was previously prepared, the tibia and polyethylene trials were placed. Once the trial talar and polyethylene components were placed (Fig. 9), the tibiotalar joint was assessed for adequate sagittal motion, coronal stability, and alignment. The trial TATTR was also assessed for varus/valgus stability and that the implants remained located in the tibiotalar, subtalar, and talonavicular joints. Fluoroscopic images were taken to assess the appropriateness of the size of the talar component. If the talar component seems too large and the ankle is not able to be dorsiflexed past neutral, then the surgeon should trial with the smaller talar component.

Once appropriate stability and alignment were confirmed, the trial components are removed and the ankle was thoroughly irrigated. The final talar component was placed first, followed by the tibia component.

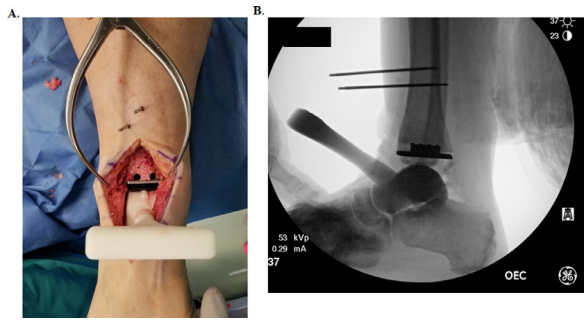

Fig. 9. Trial talar component. Intraoperative clinical (*A*) and fluoroscopic lateral (*B*) view of the ankle with the trial total talus component. Note the appropriate length of the talar component and proper seating within the subtalar joint without talonavicular subluxation

The polyethylene size was again trialed before choosing the final polyethylene bearing. Next, final fluoroscopic images were taken (Fig. 10). The wound is then irrigated for a final time and the capsule was closed with size 0 braided absorbable suture. The extensor retinaculum was then closed with interrupted size 2-0 braided absorbable suture. The dermis was closed with a size 4-0 braided absorbable suture while the skin was approximated using an unbraided size 3-0 nonabsorbable suture in a mattress fashion. Soft dressings were then placed and a well-padded short leg splint is applied. Technical pearls and pitfalls can be found on Table 3.

Postoperative Course

The patient was made nonweight bearing for the first 2 weeks to allow for adequate wound healing and soft tissue healing around the implants. At 3 weeks, the splint and dressings were removed and the patient was placed into a controlled ankle motion (CAM) boot with progressive weightbearing over the next 6 weeks. During this period, the patient was allowed to remove the CAM boot to perform ankle range of motion exercises. At 8 weeks, the patient's CAM boot was discontinued and formal physical therapy was initiated to work on gait training. At her most recent follow-up at 1 year, the patient was doing well with 1/10 pain and was walking a half of a mile daily. Clinically, she had 15° of passive tibiotalar dorsiflexion and 40° plantarflexion. She was overall satisfied with her procedure. Standing plain radiographs of her left ankle revealed maintained ankle alignment and TATTR position without complication (Fig. 11).

Discussion

We presented a case of a patient with a history of IgG deficiency and chronic steroid use that underwent a combined TATTR utilizing a

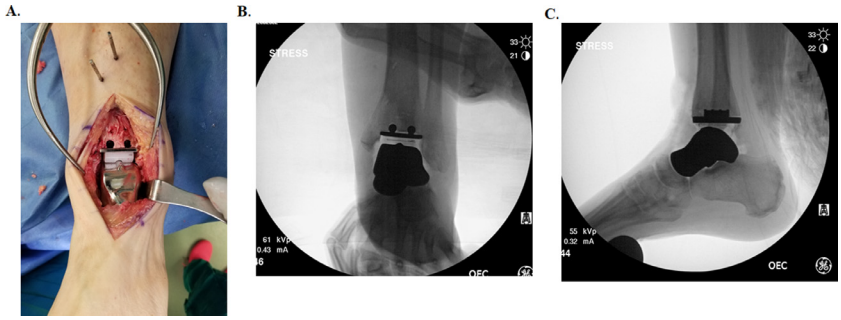

Fig. 10. Final TATTR components. Intraoperative clinical placement of the TATTR and poly liner (*A*), as well as fluoroscopic mortise (*B*), and lateral views (*C*)

Table 3
Technical pearls and pitfalls

Technical pearls and pitfalls
• Combined TATTR is a surgical option for patients with tibiotalar arthritis and talar bone collapse that have failed conservative treatment.
• Preoperative planning including bilateral 3D reconstruction CT scans is crucial for preoperative planning for the total talus prosthesis.
• If bilateral talar bone loss is evident on preoperative CT imaging, appropriate sizing of the talus prosthesis may be difficult and warrants several total talus prosthesis options to avoid intraoperative challenges with component insertion.
• Specifications for the planned total ankle tibial prosthesis should be given to the total talus prosthesis design team so that the total talus prosthesis matches the articulation of the total ankle tibia and polyethylene liner.
• Be sure to remove all bony debris from the subtalar joint after the native talus is removed to ensure proper positioning of the trial and final total talus prosthesis.
• Unlike isolated TTR, the tibial resection during the combined TATTR should make it easier to place the TATTR components. However, consider a tendo achilles lengthening procedure if neutral dorsiflexion cannot be achieved. Also, consider complete relaxation from anesthesia if the talar component is difficult to insert.
• Intraoperative range of motion and prosthesis stability should be heavily scrutinized for both the trial and final components. Appropriate sizing of the components should also be confirmed under fluoroscopic imaging.
• Postoperative recovery is prolonged and close clinical and radiographic follow-up to assess prosthesis stability is required.
• Lifetime activity modifications to avoid high-impact and strenuous activities to reduce the risk of early prosthesis failure.

Cobalt-Chromium-Molybdenum tibial STAR component, mobile-bearing polyethylene liner, and 3D additive Cobalt-Chromium custom TTR. The goal of performing a TATTR is to provide pain relief while retaining motion at the tibiotalar, talonavicular, and possibly subtalar joints; improve the patient's functional status; minimize limb shortening; and restore hindfoot alignment. At 1-year follow-up, the patient successfully returns to activities of daily living without complication.

The outcomes following TTR have improved with the evolution of TTR design and biomaterials (20,21,30). Early talar body prosthesis had universally poor results (18). Harnroongroj et al reported on 36 first and second generation stainless-steel partial talar body prosthesis from 1974 to 2011 for mostly traumatic talar AVN (20). At a mean follow-up of 23.5 years, 20 of the 28 still functional prostheses could ambulate for up to 1 hour with minimal pain and 26 of 28 patients had a plantigrade foot position. The mean American Orthopaedic Foot and Ankle Score (AOFAS) was 74.3 at final follow-up. Complications included size mismatch (n = 2), infection (n = 1), tumor recurrence (n = 2), and AVN of the talar neck (n = 1). These complications were treated with conversion to tibiotalar arthrodesis (n = 3), prosthesis revision (n = 1), and below-the-knee amputation (n = 1). Taniguchi et al performed a retrospective study on 22 patients undergoing first and second-generation ceramic partial talar body prosthesis for AVN of the talus from 1999 to 2006. At a mean follow-up of 96 months, the first-generation ceramic partial talar body prosthesis group (n = 8) had improvement of the AOFAS score from 46.6 to 80.0. However, all first-generation prostheses (n = 8) had radiographic evidence of talar neck AVN and implant loosening. There were 2 revisions to TTR in this group. In the second-generation ceramic partial talar body prosthesis group (n = 14), the mean AOFAS score improved from 50.4 to 81.1 at a mean follow-up of 83 months. There were 4 patients with talar neck fracture and prosthesis loosening that underwent conversion to TTR.

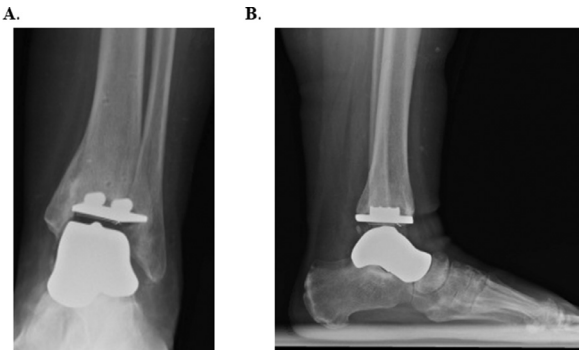

Fig. 11. Plain Radiographs of TATTR components at 1-year follow-up. Postoperative standing AP (*A*) and lateral (*B*) plain radiographs of the left ankle. The TATTR components were well-positioned without evidence of failure

The development of third-generation total talus prosthesis has shown some favorable short-term outcomes. Taniguchi et al reported on 51 patients (55 ankles) that underwent ceramic TTR from 2005 to 2012 for talar AVN (21). At a mean follow-up of 52.8 months, the Japanese Society for Surgery of the Foot (JSSF) Ankle-Hindfoot Scale improved for pain (15-34), function (21.2-45.1), alignment (6.0-9.8), and total (43.1-89.4). Katsui et al recently published on 6 patients (6 ankles) that underwent ceramic TTR for comminuted talar dome fractures (22). At a mean follow-up of 46.8 months, the postoperative range of motion was 10° of dorsiflexion and 31° of plantarflexion. The mean postoperative AOFAS was 78.8 and 3 patients returned to sporting activity. Two patients eventually underwent tibial component placement for progression of tibiotalar arthritis.

The most recent evolution in TTR is the evolution of 3D metal additive manufacturing. Metal additive manufacturing utilizes sequential layering of metal alloy onto a digital model to create implants that closely replicates the patient's native anatomy (13). Additive technology differs from the traditional formative (casting) or subtractive (forging, welding, and milling) manufacturing in that there is no excessive heating or wasting of metal substrate that can lead to a biomechanically weaker product (13). Compared to ceramic TTR, metal-alloy components are less brittle and have a lower susceptibility for catastrophic fracture (31). Despite these biomechanical differences between implant material, the outcomes data for 3D additive metal TTR is yet to be elucidated in the literature. Tracey et al compared the pre and postoperative radiographic foot alignment of 14 patients undergoing a 3D-printed metal TTR (30). At a mean follow-up of 20.5 weeks, they found significant improvements in both talar height and talar inclination. Long-term follow-up of patients with 3D additive TTR is needed to determine whether the improved biomechanical features leads to favorable outcomes.

The data on the utilization of combined TATTR is also limited to a few case series. Kanzaki et al performed 22 combined ceramic TATTR with primary degenerative arthritis (n = 18) rheumatoid arthritis (n = 3), and idiopathic talar AVN (n = 1) (26). At a mean follow-up of 34.9 months, postoperative range of motion improved from 26.6° to 46.5°. The postoperative JSSF Ankle-Hindfoot Scale improved for pain (17.5-35.7), function (28.0-46.0), alignment (5.0-9.7), and total (50.5-91.5). Complications included 1 intraoperative medial malleolus fracture, 2 postoperative medial malleolus fractures, and 3 cases of delayed wound healing. Kurokawa et al performed a comparative retrospective study on 10 patients undergoing combined ceramic TATTR for talar bone loss. The TATTR group was matched-paired with 10 patients undergoing standard ceramic TAR (25). At a mean follow-up of 58 months, the JSSF Ankle-Hindfoot total score improved for the TATTR group (44-89) and TAR group (49-72). The authors concluded that the combined TATTR resulted in better short-term clinical results than the standard TAR.

In conclusion, the combined 3D custom TATTR is used for patients with an unreconstructable talus and adjacent tibial plafond degeneration. The goal of performing a TATTR is to provide pain relief, retain motion at the tibiotalar joint, maintain or improve the patient's functional status, and minimize limb shortening.

References

1. Hawkins LG. Fractures of the neck of the talus. J Bone Jt Surg Am Vol 1970;52:991.
2. Vallier HA, Nork SE, Barei DP, Benirschke SK, Sangeorzan BJ. Talar neck fractures: results and outcomes. J Bone Jt Surg Am Vol 1616;86:2004.
3. Gross CE, Haughom B, Chahal J, Holmes GB Jr.. Treatments for avascular necrosis of the talus: a systematic review. Foot Ankle Spec 2014;7:387.
4. Sultan AA, Mont MA. Core decompression and bone grafting for osteonecrosis of the talus: a critical analysis of the current evidence. Foot Ankle Clin 2019;24:107.
5. Nunley JA, Hamid KS. Vascularized pedicle bone-grafting from the cuboid for Talar osteonecrosis: results of a novel salvage procedure. J Bone Jt Surg Am Vol 2017;99:848.
6. Lachman JR, Adams SB. Tibiotalocalcaneal arthrodesis for severe talar avascular necrosis. Foot Ankle Clin 2019;24:143.
7. Kitaoka HB, Patzer GL. Arthrodesis for the treatment of arthrosis of the ankle and osteonecrosis of the talus. J Bone Jt Surg Am 1998;80:370.
8. Bussewitz B, DeVries JG, Dujela M, McAlister JE, Hyer CF, Berlet GC. Retrograde intramedullary nail with femoral head allograft for large deficit tibiotalocalcaneal arthrodesis. Foot Ankle Int 2014;35:706.
9. Jeng CL, Campbell JT, Tang EY, Cerrato RA, Myerson MS. Tibiotalocalcaneal arthrodesis with bulk femoral head allograft for salvage of large defects in the ankle. Foot Ankle Int 2013;34:1256.
10. Urquhart MW, Mont MA, Michelson JD, Krackow KA, Hungerford DS. Osteonecrosis of the talus: treatment by hindfoot fusion. Foot Ankle Int 1996;17:275.
11. Boden KA, Weinberg DS, Vallier HA. Complications and functional outcomes after pantalar dislocation. J Bone Jt Surg Am 2017;99:666.
12. Michalski MH, Ross JS. The shape of things to come: 3D printing in medicine. JAMA 2014;312:2213.
13. Katsuura Y, Qureshi SA. Additive manufacturing for metal applications in orthopaedic surgery. J Am Acad Orthop Surg 2020;28:e349.
14. Hamid KS, Parekh SG, Adams SB. Salvage of severe foot and ankle trauma with a 3D printed scaffold. Foot Ankle Int 2016;37:433.
15. Nwankwo EC, Chen F, Nettles DL, Adams SB. Five-year follow-up of distal tibia bone and foot and ankle trauma treated with a 3D-printed titanium cage. Case Rep Orthoped 2019;2019:7571013.
16. Dekker TJ, Steele JR, Federer AE, Hamid KS, Adams SB Jr.. Use of patient-specific 3D-printed titanium implants for complex foot and ankle limb salvage, deformity correction, and arthrodesis procedures. Foot Ankle Int 2018;39:916.
17. Taniguchi A, Tanaka Y. An alumina ceramic total talar prosthesis for avascular necrosis of the talus. Foot Ankle Clin 2019;24:163.
18. Harnroongroj T, Vanadurongwan V. The talar body prosthesis. J Bone Jt Surg Am Vol 1997;79:1313.
19. Taniguchi A, Takakura Y, Sugimoto K, Hayashi K, Ouchi K, Kumai T, Tanaka Y. The use of a ceramic talar body prosthesis in patients with aseptic necrosis of the talus. J Bone Jt Surg Br 2012;94:1529.
20. Harnroongroj T, Harnroongroj T. The talar body prosthesis: results at ten to thirty-six years of follow-up. J Bone Jt Surg Am 2014;96:1211.
21. Taniguchi A, Takakura Y, Tanaka Y, Kurokawa H, Tomiwa K, Matsuda T, Kumai T, Sugimoto K. An alumina ceramic total talar prosthesis for osteonecrosis of the talus. J Bone Jt Surg Am 2015;97:1348.
22. Katsui R, Takakura Y, Taniguchi A, Tanaka Y. Ceramic artificial talus as the initial treatment for comminuted talar fractures. Foot Ankle Int 2020;41:79.
23. Magnan B, Facci E, Bartolozzi P. Traumatic loss of the talus treated with a talar body prosthesis and total ankle arthroplasty. a case report. J Bone Jt Surg Am 1778; 86:2004.
24. Angthong C. Anatomic total talar prosthesis replacement surgery and ankle arthroplasty: an early case series in Thailand. Orthop Rev 2014;6:5486.
25. Kurokawa H, Taniguchi A, Morita S, Takakura Y, Tanaka Y. Total ankle arthroplasty incorporating a total talar prosthesis: a comparative study against the standard total ankle arthroplasty. Bone Jt J 2019;101-b:443.
26. Kanzaki N, Chinzei N, Yamamoto T, Yamashita T, Ibaraki K, Kuroda R. Clinical outcomes of total ankle arthroplasty with total talar prosthesis. Foot Ankle Int 2019; 40:948.
27. Lee MG, JP. *Complications in Foot and Ankle Surgery: Management Strategies*. 1st ed., Springer, New York, NY, 2017.
28. Raikin SM, Kane J, Ciminiello ME. Risk factors for incision-healing complications following total ankle arthroplasty. J Bone Jt Surg Am 2010;92:2150.
29. Lazarides AL, Vovos TJ, Reddy GB, DeOrio JK, Easley ME, Nunley JA, Adams SB. Algorithm for management of periprosthetic ankle fractures. Foot Ankle Int 2019;40:615.
30. Tracey J, Arora D, Gross CE, Parekh SG. Custom 3D-printed total talar prostheses restore normal joint anatomy throughout the hindfoot. Foot Ankle Special 2019;12:39.
31. Abdel MP, Heyse TJ, Elpers ME, Mayman DJ, Su EP, Pellicci PM, Wright TM, Padgett DE. Ceramic liner fractures presenting as squeaking after primary total hip arthroplasty. J Bone Jt Surg Am 2014;96:27.